ASTEROID AND COMET ORBITS USING RADAR DATA

D. K. YEOMANS, P. W. CHODAS, M. S. KEESEY, AND S. J. OSTRO
Jet Propulsion Laboratory, California Institute of Technology, Pasadena, California 91109

J. F. CHANDLER AND I. I. SHAPIRO
Harvard–Smithsonian Center for Astrophysics, 60 Garden Street, Cambridge, Massachusetts 02138
Received 23 July 1991; revised 20 September 1991

ABSTRACT

For the 30 asteroids and 4 comets for which radar astrometric data were given by Ostro [AJ, 102, 1490 (1991b)], orbits have been computed using both the radar and the existing optical measurements. The techniques required to process radar data in orbit determination solutions are outlined and future radar observation opportunities for asteroids and comets are identified. For asteroids and comets that have only short intervals of optical astrometric data, the additional use of only a few radar observations allows a far more accurate extrapolation of their future motions. The use of radar data can often ensure an object's successful recovery at future Earth returns and greatly assist efforts in monitoring the motions of the rapidly growing population of known near-Earth objects, including their future close-Earth approaches.

1. INTRODUCTION

Since the first radar observations of asteroid 1566 Icarus in June 1968, there have been successful radar experiments involving over 60 different mainbelt and near-Earth asteroids (Ostro 1989; Ostro *et al.* 1991b). Although the focus of these radar experiments has been to infer the asteroids' physical characteristics from the properties of the returned signals, corrections to the predicted Doppler and/or time delay ephemerides are also obtained. The measured differences between received and transmitted frequencies (Doppler shifts) and the round-trip time delays can provide extremely powerful data types for the orbit determination of asteroids and comets (Yeomans *et al.* 1987).

Astrometric radar data were first used to refine the orbit of an asteroid with the radar observations of Icarus in 1968. Shapiro *et al.* (1968) and Shapiro *et al.* (1971) included radar data in their orbital analysis of Icarus to compare the perihelion advance with the prediction from general relativity. Lieske & Null (1969) also included radar data in their orbit determination for Icarus. But it was more than two decades before "radar" orbits were published for other Earth-approaching asteroids: 1986 JK (Ostro *et al.* 1989), 1989 PB (Ostro *et al.* 1990b), 1627 Ivar (Ostro *et al.* 1990a), and 1986 DA (Ostro *et al.* 1991a). Using the available optical and radar data, Yeomans (1991) presented orbits for a dozen near-Earth asteroids that were considered by Weissman *et al.* (1989) to be extinct comets. For at least one of these objects, Icarus, the inclusion of a cometlike, outgassing acceleration model was required to fit the observations successfully.

By outlining the techniques required to process radar data in the asteroid and comet orbit determination process, we hope to facilitate the future use of these measurements. In Sec. 2, we first outline a procedure that can be used to compute light time corrections for the radar data. A discussion of the partial derivatives required to improve the initial conditions in the weighted least squares orbit computation process is also given and station locations are presented for the observatories that have provided radar data. Section 3 presents improved orbits for the 30 asteroids and 4 comets for which radar astrometry has been published by Ostro *et al.* (1991b). Section 4 presents a discussion of radar measurements as a powerful astrometric data type and a list of future radar observing opportunities (1991–1996) when asteroids and comets come within 0.3 AU of the Earth.

2. RADAR MEASUREMENTS IN THE ORBIT DETERMINATION PROCESS

Two types of radar measurements are useful for orbit determination: time delay and Doppler frequency shift (Ostro *et al.* 1991b). Time delay is a measurement of the round-trip light time of the signal, from the time it leaves the transmitter to the time it arrives at the receiver. The Doppler frequency shift ("Doppler") is a measurement of the change in frequency from the transmitted to the received signal. Time delay is thus a measure of the distance to the asteroid, and the Doppler shift a measure of the rate of change of this distance. Both measurement types provide orbit information complementary to that of optical measurements. Typical uncertainties for recent time delay measurements are on the order of a microsecond, corresponding to position uncertainties of much less than a kilometer.

The basic steps in the processing of radar data are the same as for optical data. Expected values of the measurements are computed using an *a priori* ephemeris of the target body. The partial derivatives ("partials") of these computed values with respect to the initial orbital elements at a fixed epoch are also computed. Residuals are then formed by subtracting the computed values of the measurements from the observed values. The radar residuals and partials are combined with the optical residuals and partials in a linearized, weighted least squares procedure to produce estimated corrections to the initial orbital elements at the epoch. These steps are repeated until the estimated corrections become sufficiently small (e.g., less than one-tenth the corresponding standard errors).

 0004-6256/92/010303-15$00.90

2.1 Radar Light-Time Solution

The reduction of radar data for use in the orbit determination process requires computations quite different from those required for traditional optical astrometry. Radar observations involve two ground-based participants, a transmitter, and a receiver which may not be at the same location. Two light-time solutions must therefore be computed, one for the "up" leg of the signal path and one for the "down" leg. Furthermore, radar measurements typically have a much higher fractional precision than optical data, requiring the use of more precise models during the data reduction. For example, effects such as the finite size of the target body and variabilities in the Earth's rotation cannot be neglected and relativistic contributions to the time delays sometimes have to be considered.

Radar measurements are modeled by computing the positions and velocities of the three participants: the transmitter at the transmit time, the surface of the asteroid or comet at the signal bounce time, and the receiver at the receive time. Since radar measurements are usually referred to the epoch of reception of the echo signal, the computation sequence works backward in time: given the receive time, the bounce time is computed iteratively, and, using this result, the transmit time is computed iteratively. The time delay for the round-trip signal is computed by summing the two time intervals. The Doppler shift for the round-trip signal is computed by summing the rates of change of the up-leg and down-leg delays and multiplying by the transmit frequency.

The precise computation of the signal delay requires three corrections. The first correction results from the general relativistic contribution to the time delay due to the Sun's gravitational field (Shapiro 1964). The second correction is included to account for the slowing of the radar signal as it passes through the Earth's atmosphere and ionosphere, and the third correction accounts for the analogous slowing of the signal in the solar corona. Procedures for applying these corrections are discussed, for example, by Standish (1990). However, for the processing of current asteroid and comet radar data, these corrections are usually much less than the errors in the delay measurements themselves.

One possible procedure for modeling radar measurements is outlined below. The method was originally developed for lunar and planetary targets (see, for example, Ash 1972; Standish 1990). The procedure can be divided into the following four steps, which, as indicated earlier, work backward in time: (1) computation of the receiver position at receive time, (2) computation of the down-leg signal path, (3) computation of the up-leg signal path, and (4) computation of expected values of the radar measurements. Figure 1 depicts the various vectors involved. Position and velocity vectors referenced to the solar system barycenter are denoted by **r** and **v**; position vectors referenced to radar antennas are denoted by **ρ**. Subscripts *r*, *t*, *s*, *e*, and *b* refer to the receiver, transmitter, Sun, Earth, and bounce point, respectively. (The bounce point is that point on the asteroid's surface from which the main part of the echo signal is reflected.) Variables written with and without boldface type are vectors and scalars, respectively. Although the radar target in this discussion is assumed to be an asteroid, the procedure applies for a comet as well.

The barycentric position r_r and velocity v_r of the receiver at receive time. The Earth-fixed geocentric position $\mathbf{R}_r$ and velocity $\mathbf{V}_r$ of the receiving antenna are computed first. Section *2.3*, below, tabulates the coordinates of all radar antennas

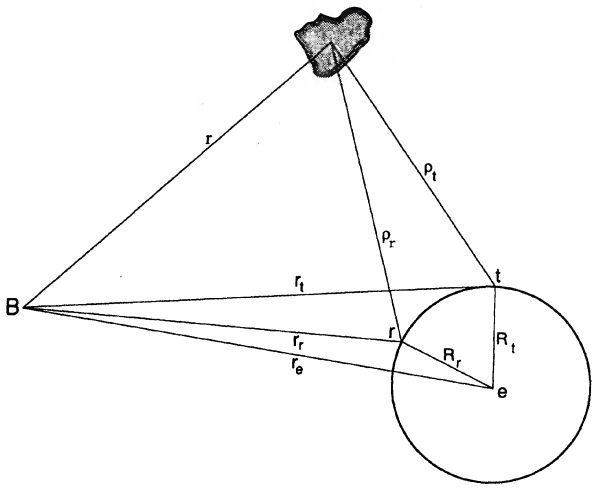

FIG. 1. A schematic diagram showing the vector relationships involved in the light-time solution. To keep the diagram relatively simple, only the Earth's rotation (and not its translational motion) is represented between the time of the radar station's transmit and receive times. The diagram shows the relative positions of the Earth's center (e), the transmit (t) and receive (r) radar stations, the irregularly shaped asteroid, and the solar system barycenter (B). The symbol "r" represents a barycentric vector but when used as a subscript, it denotes the receiving antenna.

that have provided astrometric data to date. These vectors are rotated into the inertial frame using an Earth model that takes into account the effects of polar motion, nutation, precession, and variable rotation rate (for a recent description, see Sovers & Fanselow 1987). The time offset TDB − UTC at the receive time is determined, and added to the UTC receive time to produce t_r, the receive time in barycentric dynamical time TDB. The Earth's barycentric position and velocity at the receive time, $\mathbf{r}_e(t_r)$ and $\mathbf{v}_e(t_r)$ are then obtained from a planetary ephemeris and added to the respective geocentric vectors to produce the desired barycentric position and velocity of the receiver at the receive time, $\mathbf{r}_r(t_r)$ and $\mathbf{v}_r(t_r)$, respectively.

The down-leg iteration. In this step, the bounce time t_b and the asteroid's barycentric position $\mathbf{r}(t_b)$ at the bounce time are determined through an iterative process. To start the iteration, an initial estimate of the time delay τ_D from bounce to reception (the down-leg time delay) is computed from

$$\tau_D \approx (1/c)\left[\,|\mathbf{r}(t_r) - \mathbf{r}_r(t_r)| - R_b\,\right], \tag{1}$$

where $\mathbf{r}(t_r)$ is the asteroid's barycentric position at the receive time, obtained from its ephemeris, R_b is the estimated radius of the asteroid at the bounce point, and c is the speed of light. An estimate of t_b follows from the relation

$$t_b = t_r - \tau_D. \tag{2}$$

We then obtain the barycentric position of the asteroid's center of mass at the estimated bounce time, $\mathbf{r}(t_b)$, from the asteroid's ephemeris. Using this result, we form the down-leg vector

$$\boldsymbol{\rho}_r = \mathbf{r}(t_b) - \mathbf{r}_r(t_r), \tag{3}$$

which is the estimated position of the asteroid's center of

mass relative to the receive point. We then compute an improved estimate for the down-leg delay using

$$\tau_D = (1/c)(\rho_r - R_b) + \Delta\tau_D, \tag{4}$$

where $\Delta\tau_D$ is a small correction term which includes the relativistic and media contributions to the propagation delay. Equations (2)–(4) are iterated until the latest estimate of τ_D differs from the previous estimate by less than some small value such as 0.05 μs, which is well below the delay resolution of current radar systems. Typically, only a few iterations are needed.

The up-leg iteration. A similar iterative procedure is used to find the up-leg time delay τ_U, which is the interval between the time of transmission of the signal, and the bounce time at the asteroid. We begin this iteration with the approximation

$$\tau_U \approx \tau_D, \tag{5}$$

and then estimate the transmit time t_t from the relation

$$t_t = t_b - \tau_U. \tag{6}$$

We next compute the barycentric position and velocity of the transmitter at the estimated transmit time, $\mathbf{r}_t(t_t)$ and $\mathbf{v}_t(t_t)$, using essentially the same procedure as outlined above for the down-leg iteration. We then form the corresponding estimate of the up-leg vector

$$\boldsymbol{\rho}_t = \mathbf{r}(t_b) - \mathbf{r}_t(t_t), \tag{7}$$

and use this to refine the estimate of the up-leg time delay

$$\tau_U = (1/c)(\rho_t - R_b) + \Delta\tau_U, \tag{8}$$

where $\Delta\tau_U$ is a small correction term analogous to $\Delta\tau_D$. Equations (6)–(8) are iterated as before, until convergence is achieved.

The computation of total signal delay and Doppler shift. The estimated round-trip time delay in UTC is then

$$\tau = (\tau_U + \tau_D) + (\mathrm{TDB} - \mathrm{UTC})_t - (\mathrm{TDB} - \mathrm{UTC})_r, \tag{9}$$

which is to be compared with the measured delay, obtained as a UTC time interval. The Doppler shift is proportional to the rate of change of τ, and therefore includes indirect terms due to the dependence of the bounce and transmit times on the delay. Neglecting these terms at first, as well as the time dependence of the bounce radius R_b, we compute the relative velocities of the bounce point with respect to the transmitting and receiving antennas from

$$\begin{aligned} \dot{\boldsymbol{\rho}}_t &\approx \mathbf{v}(t_b) - \mathbf{v}_t(t_t), \\ \dot{\boldsymbol{\rho}}_r &\approx \mathbf{v}(t_b) - \mathbf{v}_r(t_r), \end{aligned} \tag{10}$$

in which the barycentric velocity of the bounce point is approximated by that of the asteroid's mass center. These expressions are correct only to order v/c. The rates of change of the up-leg and down-leg distances are given by

$$\begin{aligned} \dot{\rho}_t &= (1/\rho_t)\boldsymbol{\rho}_t \cdot \dot{\boldsymbol{\rho}}_t, \\ \dot{\rho}_r &= (1/\rho_r)\boldsymbol{\rho}_r \cdot \dot{\boldsymbol{\rho}}_r. \end{aligned} \tag{11}$$

An expression for the Doppler shift accurate to second order requires not only the terms omitted in Eq. (10), but also relativistic corrections for expressing UTC in terms of the coordinate time of the ephemerides. We may write the Doppler frequency shift f_D, valid to order v^2/c^2, as (Moyer 1971; see also, Shapiro *et al.* 1966)

$$\begin{aligned} f_D = -\frac{f_T}{c}(\dot{\rho}_t + \dot{\rho}_r) - \frac{f_T}{c^2}\Bigg[\frac{\dot{\rho}_t}{\rho_t}(\boldsymbol{\rho}_t \cdot \mathbf{v}_t) - \frac{\dot{\rho}_r}{\rho_r}(\boldsymbol{\rho}_r \cdot \mathbf{v}) \\ - \dot{\rho}_t\dot{\rho}_r + GM_s\left(\frac{1}{|\mathbf{r}_t - \mathbf{r}_s|} - \frac{1}{|\mathbf{r}_r - \mathbf{r}_s|}\right) \\ + \frac{1}{2}(v_t^2 - v_r^2)\Bigg], \end{aligned} \tag{12}$$

where f_T is the transmitter frequency, GM_s is the gravitational constant times the mass of the Sun, and r_s is the barycentric position of the Sun's center of mass.

2.2 Partial Derivatives for Radar Measurements

The use of radar delay and Doppler measurements to improve an existing orbit requires the computation of the partial derivatives of the theoretical expressions for these measurements with respect to the barycentric position and velocity $(\mathbf{r}_o, \mathbf{v}_o)$ of the object at the initial epoch (t_o). Using the chain rule in vector-matrix form, we write these partial derivatives as follows:

$$\begin{aligned} \frac{\partial\tau}{\partial\mathbf{r}_o} &= \frac{\partial\tau}{\partial\mathbf{r}}\frac{\partial\mathbf{r}}{\partial\mathbf{r}_o}, \\ \frac{\partial\tau}{\partial\mathbf{v}_o} &= 0, \\ \frac{\partial f_D}{\partial\mathbf{r}_o} &= \frac{\partial f_D}{\partial\mathbf{r}}\frac{\partial\mathbf{r}}{\partial\mathbf{r}_o} + \frac{\partial f_D}{\partial\mathbf{v}}\frac{\partial\mathbf{v}}{\partial\mathbf{r}_o}, \\ \frac{\partial f_D}{\partial\mathbf{v}_o} &= \frac{\partial f_D}{\partial\mathbf{r}}\frac{\partial\mathbf{r}}{\partial\mathbf{v}_o} + \frac{\partial f_D}{\partial\mathbf{v}}\frac{\partial\mathbf{v}}{\partial\mathbf{v}_o}, \end{aligned} \tag{13}$$

where $\mathbf{r}$ and $\mathbf{v}$ are evaluated at the bounce time t_b. The second partial derivative in each term on the right is computed via numerical integration along with the equations of motion for the asteroid. The first partial derivative in each term is computed from the following analytical expressions, correct to order v/c:

$$\begin{aligned} \frac{\partial\tau}{\partial\mathbf{r}} &= \frac{1}{c}\left(\frac{1}{\rho_t}\boldsymbol{\rho}_t + \frac{1}{\rho_r}\boldsymbol{\rho}_r\right), \\ \frac{\partial f_D}{\partial\mathbf{r}} &= \frac{f_T}{c}\left[\frac{1}{\rho_t}\left(\frac{\dot{\rho}_t}{\rho_t}\boldsymbol{\rho}_t - \dot{\boldsymbol{\rho}}_t\right) + \frac{1}{\rho_r}\left(\frac{\dot{\rho}_r}{\rho_r}\boldsymbol{\rho}_r - \dot{\boldsymbol{\rho}}_r\right)\right], \\ \frac{\partial f_D}{\partial\mathbf{v}} &= -\frac{f_T}{c}\left(\frac{1}{\rho_t}\boldsymbol{\rho}_t + \frac{1}{\rho_r}\boldsymbol{\rho}_r\right) = -f_T\frac{\partial\tau}{\partial\mathbf{r}}. \end{aligned} \tag{14}$$

2.3 Radar Station Locations

Table 1 gives the Earth-fixed positions for the radar antennas that have provided astrometric data to date. Each antenna's east longitude, distance from the spin axis (d) and height above the Earth's equatorial plane (h) are listed. The coordinates of the Arecibo and Haystack antennas were derived from the information in the 1981 Astronomical Almanac (U.S. Naval Observatory, 1980), while those of the Goldstone stations were obtained from Moyer (1989).

3. ORBITS USING RADAR AND OPTICAL DATA

Asteroid and comet radar astrometric data, for 30 asteroids and 4 comets, are presented in the paper by Ostro *et al.* (1991b). For each of these objects, our Table 2 presents or-

TABLE 1. Earth-fixed coordinates for radar stations.

	East Longitude (deg.)	Distance from Spin Axis d (km)	Height above equatorial plane h (km)
Arecibo Puerto Rico	293.24692	6056.525	1994.665
Goldstone (Mars site, DSS 14) Fort Irwin, CA	243.11047	5203.997	3677.052
Goldstone (Venus site, DSS 13) Fort Irwin, CA	243.20512	5215.484	3660.957
Haystack, Westford, MA	288.51128	4700.514	4296.900

bits based upon these data and the optical data. For each object, we give the observation interval and the number of optical, Doppler, and delay measurements used in calculating the orbit. The given normalized root mean square (rms) residuals provide an indication of how well the resultant orbit represents the various observations. In computing the rms residuals, each individual residual (observed minus computed value) was normalized by dividing by its standard error. Also presented in Table 2 is the target radius assumed in the reduction of the radar measurements. Many of these radii were obtained from McFadden *et al.* (1989) and Tedesco *et al.* (1989). The radii of objects with very poorly known sizes were assumed to be 1 km; the accuracy of our orbit determination process is insensitive to errors of a few kilometers in the target radius. In weighting the optical and radar data for the orbit solutions, the optical data were assigned a standard error of 1″ and the radar data were given standard errors from Ostro *et al.* (1991b). The "radar" orbits of ten near-Earth asteroids given by Yeomans (1991) are also given in Table 2. For the orbit of 1566 Icarus, the radial nongravitational parameter, A_1 (Marsden *et al.* 1973, see Sec. 4), was included as a solution parameter along with the six orbital elements. For completeness, we have re-determined the previously published orbits for 1627 Ivar, 1986 DA, 1986 JK, and 1989 PB (Ostro *et al.* 1990a; Ostro *et al.* 1991a; Ostro *et al.* 1989; Ostro *et al.* 1990b).

The orbits presented in Table 2 were computed using a linearized weighted least squares estimation algorithm and a numerical integration scheme that used a variable step-size, variable-order Adams method (Krogh 1972). Planetary perturbations from all nine planets were taken into account at each integration time step; the Earth–Moon system was treated as one body at the barycentric location for this system. The step size varied to ensure that the estimated local error at each step was less than an input tolerance of 10^{-13} AU/day. All computations were performed in double precision, which provides 18 significant figures on JPL's Unisys computer. As a check, independent orbit determinations with similar precision, based on the same data, were made at the Center for Astrophysics for some of the objects. The partial derivatives of the theoretical expressions for the observables with respect to the relevant parameters were numerically integrated along with the object's equations of motion; these equations included general relativistic effects (see, for example, Newhall *et al.* 1983). Although the standard errors in the orbit parameters are generally much greater than the last digits shown in Table 2, some of these parameters are highly correlated and we retain the extra digits so that other solutions can be compared with ours.

4. DISCUSSION AND FUTURE PROSPECTS

Astrometric radar data provide estimates of the object's distance and velocity along the observer's line of sight, and hence these data are complementary to optical, plane-of-sky measurements. Radar data taken during an object's close approach to the Earth are most powerful, and the orbit improvement most dramatic, if the object has only a short optical astrometric history (Yeomans *et al.* 1987). A case in point is the recovery of minor planet 1989 PB by M. Hartley, S. M. Hughes, and R. McNaught at the Anglo–Australian Observatory on 1990 May 3. Using an ephemeris based upon the 65 available optical position measurements over the interval 1989 August 1–24, the predicted and observed positions of the object on 1990 May 3 differed by 37″ in right ascension and 23″ in declination. Had they access to an ephemeris based on an orbit that included the 6 Doppler and 6 delay measurements (see Table 2) in addition to the optical observations, the position differences would have been reduced to 1.″4 and 0.″8, respectively.

Using the poorly observed asteroid 1990 OS as another example, we computed an orbit using only the 27 available optical observations over the interval from 1990 July 21 to August 3, and a second that employed the two Doppler measurements on 1990 August 2–3 as well. The latter orbit is the one given in our Table 2. In mid-December 1992, when the asteroid will approach the Earth to within 0.7 AU, the predicted ephemeris positions from the two orbits differ by more than a half degree on the sky. A separate error analysis along the lines outlined by Yeomans *et al.* (1987) suggests that the predicted positions resulting from the second orbit will be good to a few arcminutes while those from the first will be at least a factor of 20 less accurate.

Radar observation residuals are typically about 1 Hz in Doppler and about a microsecond in round-trip delay time. At the Arecibo transmitter frequency (2380 MHz), these errors correspond to velocity and range errors of 6.3 cm/s and 150 m. For the Goldstone frequency (8495 MHz), the corresponding velocity error is less than 2 cm/s. The power of the radar data becomes evident when one realizes that radar measurement errors are orders of magnitude smaller than the position and velocity uncertainties inherent in orbits based only upon optical data that span only short time intervals.

Although our discussion of astrometric radar data has focused upon asteroid observations, the techniques and conclusions presented here apply for comets as well. Since the population of short-periodic comets is roughly an order of magnitude smaller than the family of near-Earth asteroids, the opportunities for cometary radar observations are relatively scarce. Beginning with the first radar observation of comet Encke in November 1980 (Kamoun *et al.* 1982a), radar signals have been successfully returned from comets P/Grigg–Skjellerup in May–June 1982 (Kamoun *et al.* 1982b), 1983 VII *IRAS*–Araki–Alcock in May 1983 (Goldstein *et al.* 1984; Harmon *et al.* 1989), and 1983 V Sugano–Saigusa–Fujikawa in June 1983 (Campbell *et al.* 1983). The orbits for these four comets in Table 2 represent the first cometary orbits to include radar data. The radial and trans-

TABLE 2. Orbital elements estimated from optical and radar astrometric data. The mean anomaly (M) is given in degrees for the stated epoch, the mean motion (n) is in degrees per day, the semimajor axis (a) and perihelion distance (q) in AU, and the osculating period (P) in years. The perihelion passage time (T) is given in Terrestrial Dynamic Time (TDT). The angular elements include the argument of perihelion (Peri.), the longitude of the ascending node (Node), and the inclination (Incl.); these elements are given in degrees, referred to the ecliptic plane and with respect to both the mean equinox of the FK5 reference star catalog at the J2000.0 epoch (FK5/J2000.0) and the mean equinox of the FK4 reference star catalog at the B1950.0 epoch. Since this latter system has had the small effects of elliptic aberration removed, it is not exactly an FK4-based system. Rather, it is consistent with JPL planetary ephemerides (i.e., DE118, DE125, and DE130). For the six orbital elements used in the orbital solutions, estimates of the standard errors are given in parentheses in units of the last decimal place given for that particular element. These estimated standard errors are based in part on comparisons with solutions made independently at the Center for Astrophysics for some of the objects and are threefold larger than statistical standard errors. Because there are high correlations between some of the elements, they are represented by more digits than are significant. High correlations occur most often between the perihelion distance and eccentricity for well observed objects and between the longitude of the ascending node and the argument of perihelion for objects whose orbits have low inclinations. An optical observation is taken to be a pair of right ascension and declination measurements for a given time.

7 Iris
Observation interval: 1901 Mar. 27 - 1989 Mar. 3
No. of astrometric observations (optical, Doppler, delay) = 2830, 0, 2
Normalized RMS (optical, Doppler, delay, total) = 0.61, -, 1.42, 0.61
Assumed radius = 96.0 km
Epoch 1991 Dec. 10.0 TDT = JD 2448600.5

			1950.0	J2000.0
M	346.185014	Peri.	144.796420 (100)	144.728861
n	0.26736773	Node	259.325464 (98)	260.091256
a	2.38632758	Incl.	5.513113 (8)	5.512495
e	0.22895613 (6)	P	3.69	
q	1.83996326 (15)	T	1992 Jan. 30.670358 (58)	

105 Artemis
Observation interval: 1912 Oct. 7 - 1989 Oct. 4
No. of astrometric observations (optical, Doppler, delay) = 83, 0, 2
Normalized RMS (optical, Doppler, delay, total) = 1.21, -, 0.16, 1.20
Assumed radius = 61.5 km
Epoch 1991 Dec. 10.0 TDT = JD 2448600.5

			1950.0	J2000.0
M	352.220984	Peri.	55.999194 (375)	55.995177
n	0.26966266	Node	187.844389 (272)	188.546672
a	2.37276927	Incl.	21.490969 (95)	21.484618
e	0.17651677 (104)	P	3.65	
q	1.95393570 (44)	T	1992 Jan. 7.847212 (1062)	

433 Eros
Observation interval: 1930 Sep. 29 - 1989 Feb. 1
No. of astrometric observations (optical, Doppler, delay) = 1362, 3, 1
Normalized RMS (optical, Doppler, delay, total) = 0.87, 0.94, 0.51, 0.87
Assumed radius = 10.5 km
Epoch 1991 Dec. 10.0 TDT = JD 2448600.5

			1950.0	J2000.0
M	209.789425	Peri.	178.584444 (46)	178.557456
n	0.55966332	Node	303.738295 (32)	304.463348
a	1.45831548	Incl.	10.826633 (11)	10.830732
e	0.22286947 (3)	P	1.76	
q	1.13330149 (4)	T	1992 Sep. 3.394532 (34)	

TABLE 2. (continued)

654 Zelinda
Observation interval: 1908 Jan. 4 - 1988 Jan. 20
No. of astrometric observations (optical, Doppler, delay) = 76, 0, 2
Normalized RMS (optical, Doppler, delay, total) = 1.17, —, 0.64, 1.16
Assumed radius = 66.0 km
Epoch 1991 Dec. 10.0 TDT = JD 2448600.5

			1950.0	J2000.0
M	24.008773	Peri.	213.714350 (315)	213.693946
n	0.28301921	Node	277.968702 (269)	278.686638
a	2.29751729	Incl.	18.126129 (99)	18.127615
e	0.23070390 (57)	P	3.48	
q	1.76747105 (132)	T	1991 Sep. 16.169104 (462)	

1036 Ganymed
Observation interval: 1941 May 20 - 1989 June 4
No. of astrometric observations (optical, Doppler, delay) = 337, 1, 0
Normalized RMS (optical, Doppler, delay, total) = 0.96, 0.48, -, 0.96
Assumed radius = 20.5 km
Epoch 1991 Dec. 10.0 TDT = JD 2448600.5

			1950.0	J2000.0
M	164.883782	Peri.	131.887406 (111)	131.877901
n	0.22653793	Node	215.341766 (98)	216.048819
a	2.66507087	Incl.	26.481709 (48)	26.476755
e	0.53709819 (24)	P	4.35	
q	1.23366613 (64)	T	1989 Dec. 12.158172 (222)	

1566 Icarus
Observation interval: 1949 June 27 - 1987 Aug. 28
No. of astrometric observations (optical, Doppler, delay) = 475, 9, 0
Normalized RMS (optical, Doppler, delay, total) = 1.04, 1.60, -, 1.05
Assumed radius = 0.9 km
Epoch 1991 Dec. 10.0 TDT = JD 2448600.5

			1950.0	J2000.0
M	33.392340	Peri.	31.195716 (85)	31.212462
n	0.88058839	Node	87.485016 (18)	88.168134
a	1.07800493	Incl.	22.886759 (80)	22.886455
e	0.82679722 (39)	P	1.12	
q	0.18671345 (42)	A1 = -1.432 (156) x 10^{-10} AU/(day)^2		
T	1991 Nov. 2.079514 (81)			

1580 Betulia
Observation interval: 1950 May 22 - 1989 June 5
No. of astrometric observations (optical, Doppler, delay) = 128, 4, 2
Normalized RMS (optical, Doppler, delay, total) = 1.14, 1.52, 0.56, 1.14
Assumed radius = 3.7 km
Epoch 1991 Dec. 10.0 TDT = JD 2448600.5

			1950.0	J2000.0
M	285.883026	Peri.	159.267695 (163)	159.275293
n	0.30318077	Node	61.697986 (17)	62.391866
a	2.19449680	Incl.	52.115829 (149)	52.118388
e	0.49021728 (23)	P	3.25	
q	1.11871656 (51)	T	1992 Aug. 10.464630 (153)	

TABLE 2. (continued)

1620 Geographos
Observation interval: 1951 Aug. 31 - 1986 Dec. 2
No. of astrometric observations (optical, Doppler, delay) = 576, 1, 1
Normalized RMS (optical, Doppler, delay, total) = 0.96, 0.16, 1.20, 0.96
Assumed radius = 1.0 km
Epoch 1991 Dec. 10.0 TDT = JD 2448600.5

			1950.0	J2000.0
M	60.085417	Peri.	276.638281 (203)	276.629486
n	0.70972570	Node	336.685965 (176)	337.393068
a	1.24473154	Incl.	13.320375 (258)	13.326572
e	0.33538510 (9)	P	1.39	
q	0.82726713 (11)	T	1991 Sep. 16.339945 (243)	

1627 Ivar
Observation interval: 1929 Sep. 25 - 1990 Aug. 26
No. of astrometric observations (optical, Doppler, delay) = 279, 1, 1
Normalized RMS (optical, Doppler, delay, total) = 1.07, 0.01, 0.33, 1.06
Radar data given with respect to object's center of mass.
Epoch 1991 Dec. 10.0 TDT = JD 2448600.5

			1950.0	J2000.0
M	186.817759	Peri.	167.386415 (119)	167.416230
n	0.38745115	Node	132.627633 (97)	133.296687
a	1.86348005	Incl.	8.447157 (29)	8.442326
e	0.39688083 (18)	P	2.54	
q	1.12390053 (33)	T	1993 Feb. 28.978260 (88)	

1685 Toro
Observation interval: 1948 July 17 - 1989 Feb. 13
No. of astrometric observations (optical, Doppler, delay) = 166, 2, 4
Normalized RMS (optical, Doppler, delay, total) = 1.12, 0.82, 0.77, 1.11
Assumed radius = 6.1 km
Epoch 1991 Dec. 10.0 TDT = JD 2448600.5

			1950.0	J2000.0
M	358.430520	Peri.	126.863959 (240)	126.824423
n	0.61661651	Node	273.754015 (243)	274.491568
a	1.36707586	Incl.	9.374070 (52)	9.375087
e	0.43577945 (35)	P	1.60	
q	0.77133230 (47)	T	1991 Dec. 12.545310 (49)	

1862 Apollo
Observation interval: 1932 Apr. 27 - 1989 Dec. 29
No. of astrometric observations (optical, Doppler, delay) = 104, 8, 4
Normalized RMS (optical, Doppler, delay, total) = 1.47, 0.34, 1.22, 1.44
Assumed radius = 0.75 km
Epoch 1991 Dec. 10.0 TDT = JD 2448600.5

			1950.0	J2000.0
M	101.539337	Peri.	285.551014 (211)	285.589271
n	0.55242802	Node	35.304762 (210)	35.965286
a	1.47102115	Incl.	6.349916 (87)	6.354875
e	0.56024560 (12)	P	1.78	
q	0.64688802 (18)	T	1991 June 9.194450 (26)	

TABLE 2. (continued)

1866 Sisyphus
Observation interval: 1964 Apr. 16 - 1988 May 14
No. of astrometric observations (optical, Doppler, delay) = 142, 1, 0
Normalized RMS (optical, Doppler, delay, total) = 1.09, 0.20, -, 1.09
Assumed radius = 4.1 km
Epoch 1991 Dec. 10.0 TDT = JD 2448600.5

			1950.0	J2000.0
M	130.259675	Peri.	292.951299 (83)	292.960503
n	0.37821194	Node	63.060315 (92)	63.751929
a	1.89370600	Incl.	41.142468 (132)	41.144883
e	0.53909597 (58)	P	2.61	
q	0.87281673 (110)	T	1990 Dec. 30.590794 (139)	

1915 Quetzalcoatl
Observation interval: 1953 Mar. 9 - 1985 Mar. 23
No. of astrometric observations (optical, Doppler, delay) = 41, 1, 0
Normalized RMS (optical, Doppler, delay, total) = 1.23, 1.08, -, 1.23
Assumed radius = 0.5 km
Epoch 1991 Dec. 10.0 TDT = JD 2448600.5

			1950.0	J2000.0
M	244.781365	Peri.	347.890557 (153)	347.894574
n	0.24391792	Node	162.365703 (105)	163.060485
a	2.53692080	Incl.	20.463917 (134)	20.457550
e	0.57436648 (38)	P	4.04	
q	1.07979852 (98)	T	1993 Mar. 26.366420 (398)	

1917 Cuyo
Observation interval: 1968 Jan. 1 - 1989 Nov. 22
No. of astrometric observations (optical, Doppler, delay) = 65, 2, 0
Normalized RMS (optical, Doppler, delay, total) = 0.92, 0.28, -, 0.91
Assumed radius = 1.0 km
Epoch 1991 Dec. 10.0 TDT = JD 2448600.5

			1950.0	J2000.0
M	243.922869	Peri.	194.161523 (159)	194.157910
n	0.31284638	Node	187.818931 (111)	188.520777
a	2.14906044	Incl.	23.990919 (80)	23.984567
e	0.50523520 (27)	P	3.15	
q	1.06327945 (59)	T	1992 Dec. 15.035562 (116)	

1981 Midas
Observation interval: 1973 Mar. 6 - 1987 Sep. 27
No. of astrometric observations (optical, Doppler, delay) = 29, 1, 0
Normalized RMS (optical, Doppler, delay, total) = 1.15, 1.77, -, 1.17
Assumed radius = 1.0 km
Epoch 1991 Dec. 10.0 TDT = JD 2448600.5

			1950.0	J2000.0
M	302.207959	Peri.	267.676889 (113)	267.677189
n	0.41621851	Node	356.491744 (63)	357.190059
a	1.77659507	Incl.	39.835576 (289)	39.842093
e	0.64986030 (52)	P	2.37	
q	0.62205647 (92)	T	1992 Apr. 26.850240 (87)	

TABLE 2. (continued)

2100 Ra-Shalom
Observation interval: 1975 Oct. 3 - 1990 Sep. 10
No. of astrometric observations (optical, Doppler, delay) = 72, 2, 0
Normalized RMS (optical, Doppler, delay, total) = 1.00, 0.30, -, 1.00
Assumed radius = 1.2 km
Epoch 1991 Dec. 10.0 TDT = JD 2448600.5

			1950.0	J2000.0
M	345.993303	Peri.	355.932995 (161)	355.934893
n	1.29853600	Node	170.267292 (92)	170.964010
a	0.83208314	Incl.	15.761908 (191)	15.755409
e	0.43651290 (260)	P	0.76	
q	0.46886811 (212)	T	1991 Dec. 20.786530 (702)	

2101 Adonis
Observation interval: 1936 Feb. 12 - 1984 July 18
No. of astrometric observations (optical, Doppler, delay) = 36, 5, 0
Normalized RMS (optical, Doppler, delay, total) = 1.24, 0.38, -, 1.20
Assumed radius = 1.0 km
Epoch 1991 Dec. 10.0 TDT = JD 2448600.5

			1950.0	J2000.0
M	302.285876	Peri.	41.685553 (2190)	41.665387
n	0.38396838	Node	350.571656 (2181)	351.290362
a	1.87473148	Incl.	1.359872 (54)	1.366374
e	0.76379216 (26)	P	2.57	
q	0.44282628 (49)	T	1992 May 8.309574 (87)	

2201 Oljato
Observation interval: 1947 Dec. 14 - 1983 July 14
No. of astrometric observations (optical, Doppler, delay) = 49, 4, 0
Normalized RMS (optical, Doppler, delay, total) = 1.08, 0.21, -, 1.06
Assumed radius = 0.7 km
Epoch 1991 Dec. 10.0 TDT = JD 2448600.5

			1950.0	J2000.0
M	245.810369	Peri.	95.761377 (766)	95.908306
n	0.30713823	Node	76.366602 (763)	76.918360
a	2.17560544	Incl.	2.514720 (218)	2.515685
e	0.71095228 (20)	P	3.21	
q	0.62885380 (42)	T	1992 Dec. 15.785801 (392)	

3103 (1982 BB)
Observation interval: 1982 Jan. 21 - 1991 May 13
No. of astrometric observations (optical, Doppler, delay) = 46, 1, 0
Normalized RMS (optical, Doppler, delay, total) = 0.88, 0.15, -, 0.88
Assumed radius = 0.7 km
Epoch 1991 Dec. 10.0 TDT = JD 2448600.5

			1950.0	J2000.0
M	42.208393	Peri.	253.722352 (173)	253.735374
n	0.59111569	Node	129.257742 (149)	129.944125
a	1.40611571	Incl.	20.942847 (112)	20.938282
e	0.35454193 (75)	P	1.67	
q	0.90758874 (110)	T	1991 Sep. 29.595377 (383)	

TABLE 2. (continued)

3199 Nefertiti
Observation interval: 1982 Sep. 13 - 1990 Aug. 22
No. of astrometric observations (optical, Doppler, delay) = 86, 1, 0
Normalized RMS (optical, Doppler, delay, total) = 1.13, 0.14, -, 1.13
Assumed radius = 1.1 km
Epoch 1991 Dec. 10.0 TDT = JD 2448600.5

			1950.0	J2000.0
M	212.221793	Peri.	53.289742 (532)	53.286567
n	0.49892293	Node	339.429557 (58)	340.130766
a	1.57439514	Incl.	32.974835 (212)	32.981122
e	0.28375905 (141)	P	1.98	
q	1.12764627 (222)	T	1992 Oct. 1.194458 (514)	

3757 (1982 XB)
Observation interval: 1982 Dec. 14 - 1987 Dec. 18
No. of astrometric observations (optical, Doppler, delay) = 35, 2, 0
Normalized RMS (optical, Doppler, delay, total) = 1.20, 0.38, -, 1.19
Assumed radius = 0.25 km
Epoch 1991 Dec. 10.0 TDT = JD 2448600.5

			1950.0	J2000.0
M	215.406022	Peri.	16.789692 (271)	16.884618
n	0.39623446	Node	74.526040 (221)	75.129876
a	1.83583884	Incl.	3.873825 (47)	3.874993
e	0.44643488 (13)	P	2.49	
q	1.01625635 (23)	T	1992 Dec. 8.920250 (73)	

3908 (1980 PA)
Observation interval: 1980 Aug. 7 - 1988 Oct. 22
No. of astrometric observations (optical, Doppler, delay) = 66, 1, 6
Normalized RMS (optical, Doppler, delay, total) = 0.86, 0.86, 0.57, 0.85
Assumed radius = 1.0 km
Epoch 1991 Dec. 10.0 TDT = JD 2448600.5

			1950.0	J2000.0
M	63.557963	Peri.	125.532466 (530)	125.360396
n	0.36901493	Node	261.348054 (554)	262.218547
a	1.92504148	Incl.	2.167869 (13)	2.167486
e	0.45794596 (6)	P	2.67	
q	1.04347650 (11)	T	1991 June 20.763167 (37)	

4034 (1986 PA)
Observation interval: 1986 Aug. 2 - 1989 Mar. 26
No. of astrometric observations (optical, Doppler, delay) = 45, 1, 0
Normalized RMS (optical, Doppler, delay, total) = 0.85, 0.13, -, 0.85
Assumed radius = 1.0 km.
Epoch 1991 Dec. 10.0 TDT = JD 2448600.5

			1950.0	J2000.0
M	218.297114	Peri.	296.436640 (333)	296.446675
n	0.90312947	Node	157.458780 (340)	158.147480
a	1.05999229	Incl.	11.172567 (117)	11.166344
e	0.44407793 (442)	P	1.09	
q	0.58927311 (425)	T	1992 May 14.902074 (1859)	

TABLE 2. (continued)

4544 (1989 FB)
Observation interval: 1989 Mar. 31 - 1991 Mar. 21
No. of astrometric observations (optical, Doppler, delay) = 43, 1, 0
Normalized RMS (optical, Doppler, delay, total) = 0.95, 0.30, -, 0.95
Assumed radius = 1.0 km
Epoch 1991 Dec. 10.0 TDT = JD 2448600.5

			1950.0	J2000.0
M	34.382996	Peri.	333.558830 (373)	333.571621
n	0.92624689	Node	23.455949 (218)	24.142090
a	1.04228113	Incl.	14.141503 (283)	14.147224
e	0.25045603 (609)	P	1.06	
q	0.78123554 (539)	T	1991 Nov. 2.879232 (911)	

4769 (1989 PB)
Observation interval: 1989 Aug. 1 - 1990 May 4
No. of astrometric observations (optical, Doppler, delay) = 70, 6, 6
Normalized RMS (optical, Doppler, delay, total) = 0.91, 0.40, 1.20, 0.91
Radar data given with respect to object's center of mass.
Epoch 1991 Dec. 10.0 TDT = JD 2448600.5

			1950.0	J2000.0
M	335.644644	Peri.	121.191228 (174)	121.170331
n	0.89908133	Node	325.095425 (56)	325.814616
a	1.06317167	Incl.	8.888399 (92)	8.894062
e	0.48314641 (52)	P	1.10	
q	0.54950409 (93)	T	1992 Jan. 6.089157 (1937)	

1986 DA
Observation interval: 1986 Feb. 5 - 1986 Aug. 16
No. of astrometric observations (optical, Doppler, delay) = 135, 1, 1
Normalized RMS (optical, Doppler, delay, total) = 0.98, 1.26, 0.00, 0.98
Radar data given with respect to object's center of mass.
Epoch 1991 Dec. 10.0 TDT = JD 2448600.5

			1950.0	J2000.0
M	72.176771	Peri.	126.779621 (561)	126.861245
n	0.20802145	Node	64.447488 (473)	65.064639
a	2.82096244	Incl.	4.292489 (31)	4.294761
e	0.58233314 (419)	P	4.74	
q	1.17822253 (31)	T	1990 Dec. 28.032072 (25776)	

1986 JK
Observation interval: 1986 May 4 - 1986 Oct. 30
No. of astrometric observations (optical, Doppler, delay) = 66, 11, 0
Normalized RMS (optical, Doppler, delay, total) = 0.96, 0.69, -, 0.94
Assumed radius = 1.0 km
Epoch 1991 Dec. 10.0 TDT = JD 2448600.5

			1950.0	J2000.0
M	58.444818	Peri.	232.425876 (344)	232.586936
n	0.21059627	Node	62.179896 (317)	62.717494
a	2.79792200	Incl.	2.138866 (83)	2.141382
e	0.68033815 (960)	P	4.68	
q	0.89438891 (238)			
T	1991 Mar. 7.479329 (70537)			

TABLE 2. (continued)

1989 JA
Observation interval: 1989 Apr. 6 - 1989 Nov. 29
No. of astrometric observations (optical, Doppler, delay) = 51, 5, 0
Normalized RMS (optical, Doppler, delay, total) = 1.31, 0.57, -, 1.29
Assumed radius = 1.0 km
Epoch 1991 Dec. 10.0 TDT = JD 2448600.5

			1950.0	J2000.0
M	9.927329	Peri.	231.825523 (354)	231.848220
n	0.41843944	Node	60.947528 (261)	61.624173
a	1.77030313	Incl.	15.228053 (538)	15.230691
e	0.48420832 (1985)	P	2.36	
q	0.91310763 (343)	T	1991 Nov. 16.275352 (44870)	

1990 MF
Observation interval: 1990 June 14 - 1990 Dec. 7
No. of astrometric observations (optical, Doppler, delay) = 39, 10, 6
Normalized RMS (optical, Doppler, delay, total) = 0.93, 0.62, 0.19, 0.87
Assumed radius = 1.0 km
Epoch 1991 Dec. 10.0 TDT = JD 2448600.5

			1950.0	J2000.0
M	208.096630	Peri.	113.848139 (972)	113.732447
n	0.42678531	Node	209.916888 (963)	210.731064
a	1.74714818	Incl.	1.862958 (8)	1.857629
e	0.45571160 (104)	P	2.31	
q	0.95095249 (38)	T	1990 Aug. 9.409111 (85)	

1990 OS
Observation interval: 1990 July 21 - 1990 Aug. 3
No. of astrometric observations (optical, Doppler, delay) = 27, 2, 0
Normalized RMS (optical, Doppler, delay, total) = 1.24, 0.34, -, 1.22
Assumed radius = 1.0 km
Epoch 1991 Dec. 10.0 TDT = JD 2448600.5

			1950.0	J2000.0
M	203.401710	Peri.	19.808584 (16771)	19.766380
n	0.45268185	Node	347.553691 (13529)	348.294432
a	1.67986351	Incl.	1.110255 (248)	1.116723
e	0.46322065 (6644)	P	2.18	
q	0.90171604 (1297)	T	1990 Sep. 16.674029 (3793)	

P/Encke
Observation interval: 1980 Aug. 13 - 1990 Oct. 1
No. of astrometric observations (optical, Doppler, delay) = 77, 1, 0
Normalized RMS (optical, Doppler, delay, total) = 1.23, 2.66, -, 1.24
Assumed radius = 1.0 km
Epoch 1994 Feb. 17.0 TDT = JD 2449400.5
T 1994 Feb. 9.475678 (1102) TDT

			1950.0	J2000.0
q	0.33091597 (238)	Peri.	186.281973 (734)	186.270793
e	0.85021339 (151)	Node	334.019828 (580)	334.729312
P	3.28	Incl.	11.934965 (209)	11.941061

A1 = -4.579 (4.143) x 10^{-10} AU/(day)^2
A2 = -2.147 (0.121) x 10^{-11} AU/(day)^2

TABLE 2. (continued)

P/Grigg-Skjellerup
Observation interval: 1961 Nov. 10 - 1988 Sep. 11
No. of astrometric observations (optical, Doppler, delay) = 107, 1, 0
Normalized RMS (optical, Doppler, delay, total) = 1.09, 0.36, -, 1.09
Assumed radius = 1.0 km
Epoch 1992 Aug. 6.0 TDT = JD 2448840.5
T 1992 July 22.137663 (704) TDT

			1950.0	J2000.0
q	0.99468958 (64)	Peri.	359.275971 (311)	359.264863
e	0.66432529 (50)	Node	212.631517 (171)	213.340425
P	5.10	Incl.	21.104159 (82)	21.099010

A1 = 7.216 (14505) x 10^{-11} AU/(day)^2
A2 = -1.147 (122) x 10^{-11} AU/(day)^2

IRAS-Araki-Alcock
Observation interval: 1983 Apr. 27 - 1983 Oct. 4
No. of astrometric observations (optical, Doppler, delay) = 230, 1, 0
Normalized RMS (optical, Doppler, delay, total) = 1.37, 0.06, -, 1.36
Assumed radius = 1.0 km
Epoch 1983 Nov. 2.0 TDT = JD 2445640.5
T 1983 May 21.253031 (282) TDT

			1950.0	J2000.0
q	0.99137925 (52)	Peri.	192.846567 (311)	192.852048
e	0.98977405 (3671)	Node	48.406291 (22)	49.103256
		Incl.	73.245390 (391)	73.249259

Sugano-Saigusa-Fujikawa
Observation interval: 1983 May 9 - 1983 June 17
No. of astrometric observations (optical, Doppler, delay) = 39, 3, 0
Normalized RMS (optical, Doppler, delay, total) = 1.20, 0.22, -, 1.18
Assumed radius = 1.0 km
Epoch 1983 July 5.0 TDT = JD 2445520.5
T 1983 May 1.329334 (164) TDT

			1950.0	J2000.0
q	0.47112283 (407)	Peri.	82.171909 (600)	82.178467
e	1.00004653 (724)	Node	82.342179 (44)	83.041480
		Incl.	96.625541 (326)	96.625821

TABLE 3. Earth-approaching minor planets and comets (<0.3 AU) from August 1991 to December 1996.

Object No.	Name	Date of Close Approach (mm/dd/yy)	Minimum Distance (AU)	10 Day Bracketing of Declination Date Dec (m/d)(deg)	Date Dec (m/d)(deg)
3103	1982 BB	8/06/91	0.124	8/01 -10.	8/11 -28.
	1991 EE	9/07/91	0.055	9/02 +14.	9/12 -11.
2100	Ra-Shalom	10/13/91	0.272	10/08 -15.	10/18 -25.
	1990 VA	11/06/91	0.255	11/01 +12.	11/11 +3.
1685	Toro	1/29/92	0.291	1/24 +0.	2/03 +2.
1981	Midas	3/11/92	0.134	3/06 -8.	3/16 -48.
4341	Poseidon	4/16/92	0.227	4/11 +41.	4/21 +39.
	1990 UQ	5/19/92	0.106	5/14 +49.	5/24 +54.
1865	Cerberus	6/24/92	0.267	6/19 +71.	6/29 +83.
3757	1982 XB	11/14/92	0.222	11/09 +15.	11/19 +13.
	1990 VA	11/19/92	0.299	11/14 +1.	11/24 -7.
4179	Toutatis	12/08/92	0.024	12/03 -32.	12/13 +02.
	1989 PB	4/08/93	0.132	4/03 -28.	4/13 -43.
2062	Aten	7/31/93	0.203	7/26 +1.	8/05 -16.
2062	Aten	12/14/93	0.276	12/09 -37.	12/19 -27.
3361	Orpheus	3/02/94	0.150	2/25 -20.	3/07 -22.
	1990 VA	5/09/94	0.294	5/04 +20.	5/14 +28.
	1990 MU	5/31/94	0.114	5/26 +19.	6/05 -24.
2062	Aten	6/20/94	0.251	6/15 +44.	6/25 +29.
1620	Geographos	8/25/94	0.033	8/20 -62.	8/30 -25.
2100	Ra-Shalom	10/12/94	0.155	10/07 -34.	10/17 -60.
	1989 VA	11/15/94	0.182	11/10 +4.	11/20 -18.
2063	Bacchus	11/17/94	0.264	11/12 -20.	11/22 -11.
2102	Tantalus	1/03/95	0.258	12/27 -42.	1/06 -10.
2062	Aten	1/12/95	0.127	1/07 +14.	1/17 +36.
2340	Hathor	1/16/95	0.137	1/11 -49.	1/21 -62.
	1990 VA	4/20/95	0.259	4/15 +3.	4/25 +12.
	1991 JX	6/09/95	0.034	6/04 +19.	6/14 +38.
2062	Aten	1/24/96	0.223	1/19 +24.	1/29 +32.
	P/Honda-Mrkos-Pajdušaková	2/04/96	0.170	1/31 -6.	2/10 +7.
	1990 VA	3/30/96	0.224	3/25 -21.	4/04 -11.
2063	Bacchus	3/31/96	0.068	3/26 +64.	4/05 +43.
	1989 UQ	5/24/96	0.288	5/19 +21.	5/29 +18.
1566	Icarus	6/11/96	0.101	6/06 +16.	6/16 -19.
	1990 MU	6/18/96	0.289	6/13 +30.	6/23 +6.
	1987 PA	7/14/96	0.265	7/09 -22.	7/19 -9.
1685	Toro	8/02/96	0.221	7/28 +38.	8/07 +52.
3103	1982 BB	8/06/96	0.115	8/01 -13.	8/11 -32.
	1989 RC	9/04/96	0.286	8/30 -24.	9/09 -30.
	1989 JA	9/13/96	0.275	9/08 -77.	9/18 -79.
	1989 RS1	9/16/96	0.196	9/11 -4.	9/21 -8.
	1988 TJ1	10/22/96	0.216	10/17 +19.	10/27 +8.
	1989 UQ	10/23/96	0.150	10/18 +06.	10/28 0.
4197	1982 TA	10/25/96	0.085	10/20 +50.	10/30 +45.
3908	1980 PA	10/27/96	0.061	10/22 +26.	11/01 +35.
4179	Toutatis	11/30/96	0.035	11/25 -31.	12/05 -3.

verse nongravitational parameters (A_1, A_2) given for comets Encke and Grigg–Skjellerup are defined in Marsden *et al.* (1973). These parameters are used to model the rocketlike thrusts acting upon an active comet's nucleus as a result of its vaporizing ices. Although radar echoes were also detected from comet Halley in November 1985, the signal was probably returned from coma particles rather than the solid nucleus, and hence no astrometric measurements are available for this comet (Campbell *et al.* 1989).

The abundance of Earth-approaching asteroids insures that a few close radar targets will be available each year. Table 3 presents a summary of known asteroids and comets that will pass within 0.3 AU of the Earth within the interval from 1991 to 1996. Only objects with secure orbits have been included. For each object on the list, the date of closest approach is followed by the minimum separation distance (in AU), and the declination of the object 5 days on either side of closest approach. The latter information is useful for determining whether the object will be within the observation windows at radar observatories.

With the relatively recent realization that a large population of near-Earth asteroids are on Earth-approaching orbits, there is a critical need to accurately monitor their future motions. For the majority of these objects, the lack of long histories of optical astrometric data implies that accurate extrapolations of their motions will be achievable most readily with the use of radar data obtained in future close approaches. The successful monitoring of their future motions will, of course, depend upon a continuing program of radar observations at the Arecibo and Goldstone facilities.

Helpful discussions with E. M. Standish are gratefully acknowledged by D.K.Y. and P.W.C. A portion of the research described in this paper was carried out by the Jet Propulsion Laboratory, California Institute of Technology, under a contract with the National Aeronautics and Space Administration. The work of J.F.C. and I.I.S. was supported, in part, by NASA.

REFERENCES

Ash, M. E. 1972, Lincoln Lab. Tech. Memo 1972-5
Campbell, D. B., Harmon, J. K., Hine, A. A., Shapiro, I. I., Marsden, B. G., & Pettengill, G. H. 1983, BAAS, 15, 180
Campbell, D. B., Harmon, J. K., & Shapiro, I. I. 1989, ApJ, 338, 1094
Goldstein, R. M., Jurgens, R. F., & Sekanina, Z. 1984, AJ, 89, 1745
Harmon, J. K., Campbell, D. B., Hine, A. A., Shapiro, I. I., & Marsden, B. G. 1989, ApJ, 338, 1071
Kamoun, P. G., Campbell, D. B., Ostro, S. J., Pettengill, G. H., & Shapiro, I. I. 1982a, Sci, 216, 293
Kamoun, P. D., Pettengill, G. H., Shapiro, I. I., & Campbell, D. G. 1982b, BAAS, 14, 753
Krogh, F. T. 1972, in Lecture Notes in Mathematics (Springer, New York), Vol. 362, p. 22
Lieske, J. H., & Null, G. W. 1969, AJ, 74, 297
McFadden, L.-A., Tholen, D. J., & Veeder, G. J. 1989, in Asteroids II, edited by R. P. Binzel, T. Gehrels, and M. S. Matthews (University of Arizona Press, Tucson), pp. 442–467
Marsden, B. G., Sekanina, Z., & Yeomans, D. K. 1973, AJ, 78, 211
Moyer, T. D. 1971, Mathematical Formulation of the Double-Precision Orbit Determination Program (DPODP), JPL Technical Report No. 32-1527, p. 160
Moyer, T. D. 1989, Station Locations Sets Referred to the Radio Frame, Jet Propulsion Interoffice Memorandum No. 314.5-1334, 24 February 1989
Newhall, X. X., Standish, Jr., E. M., & Williams, J. G. 1983, A&A, 125, 150
Ostro, S. J. 1989, in Asteroids II, edited by R. P. Binzel, T. Gehrels, and M. S. Matthews (University of Arizona Press, Tucson), pp. 192–212

Ostro, S. J., Yeomans, D. K., Chodas, P. W., Goldstein, R. M., Jurgens, R. F., & Thompson, T. W. 1989, Icarus, 78, 382
Ostro, S. J., Campbell, D. B., Hine, A. A., Shapiro, I. I., Chandler, J. F., Werner, C. L., & Rosema, K. D. 1990a, AJ, 99, 2012
Ostro, S. J., Chandler, J. F., Hine, A. A., Rosema, K. D., Shapiro, I. I., & Yeomans, D. K. 1990b, Sci, 248, 1523
Ostro, S. J., Campbell, D. B., Chandler, J. F., Hine, A. A., Hudson, R. S., Rosema, K. D., & Shapiro, I. I. 1991a, Sci, 252, 1399
Ostro, S. J., Campbell, D. B., Chandler, J. F., Shapiro, I. I., Hine, A. A., Velez, R., Jurgens, R. F., Rosema, K. D., Winkler, R., & Yeomans, D. K. 1991b, AJ, 102, 1490
Shapiro, I. I. 1964, Phys. Rev. Lett., 13, 789
Shapiro, I. I., Ash, M. E., & Tausner, M. J. 1966, Phys. Rev. Lett., 17, 933
Shapiro, I. I., Ash, M. E., & Smith, W. B. 1968, Phys. Rev. Lett., 20, 1517
Shapiro, I. I., Smith, W. B., Ash, M. E., & Herrick, S. 1971, AJ, 76, 588
Sovers, O. J., & Fanselow, J. L. 1987, Observation Model and Parameter Partials for the JPL VLBI Parameter Estimation Software MASTERFIT, 1987, JPL Publication No. 83-39, Rev. 3
Standish, E. M. 1990, A&A, 233, 252
Tedesco, E. F. 1989, in Asteroids II, edited by R. P. Binzel, T. Gehrels, and M. S. Matthews (University of Arizona Press, Tucson), pp. 1090–1138
U.S. Naval Observatory 1980, The Astronomical Almanac for the Year 1981 (U.S. Government Printing Office, Washington, DC)
Weissman, P. R., A'Hearn, M. F., McFadden, L. A., & Rickman, H. 1989, in Asteroids II, edited by R. P. Binzel, T. Gehrels, and M. S. Matthews (University of Arizona Press, Tucson), pp. 880–920
Yeomans, D. K. 1991, AJ, 101, 1920
Yeomans, D. K., Ostro, S. J., & Chodas, P. W. 1987, AJ, 94, 189